Cerebral Cortex July 2012;22:1690–1697
doi:10.1093/cercor/bhr254
Advance Access publication September 12, 2011

Immunogold Detection of L-glutamate and D-serine in Small Synaptic-Like Microvesicles in Adult Hippocampal Astrocytes

L.H. Bergersen[1], C. Morland[1], L. Ormel[1], J.E. Rinholm[1], M. Larsson[1], J.F.H. Wold[1], Å.T. Røe[1], A. Stranna[1], M. Santello[2], D. Bouvier[2], O.P. Ottersen[1], A. Volterra[2] and V. Gundersen[1,3]

[1]Department of Anatomy, Centre for Molecular Biology and Neuroscience, Institute of Basic Medical Sciences, University of Oslo, 0317 Oslo, Norway, [2]Département de Biologie Cellulaire et de Morphologie, Université de Lausanne, 1005 Lausanne, Switzerland and [3]Department of Neurology, Oslo University Hospital, Rikshospitalet, 0424 Oslo, Norway

Address correspondence to V. Gundersen, Department of Anatomy and the Centre for Molecular Biology and Neuroscience, University of Oslo, PO Box 1105 Blindern, 0317 Oslo, Norway. Email: vidar.gundersen@medisin.uio.no.

Glutamate and the N-methyl-D-aspartate receptor ligand D-serine are putative gliotransmitters. Here, we show by immunogold cytochemistry of the adult hippocampus that glutamate and D-serine accumulate in synaptic-like microvesicles (SLMVs) in the perisynaptic processes of astrocytes. The estimated concentration of fixed glutamate in the astrocytic SLMVs is comparable to that in synaptic vesicles of excitatory nerve terminals (~45 and ~55 mM, respectively), whereas the D-serine level is about 6 mM. The vesicles are organized in small spaced clusters located near the astrocytic plasma membrane. Endoplasmic reticulum is regularly found in close vicinity to SLMVs, suggesting that astrocytes contain functional nanodomains, where a local Ca^{2+} increase can trigger release of glutamate and/or D-serine.

Keywords: gliotransmitter, gold particles, rat, ultrastructure

Introduction

Astrocytes contain a variety of transmitter receptors enabling them to respond to neuronal activity by increasing the intracellular Ca^{2+} concentration ($[Ca^{2+}]_i$) (Dani et al. 1992; Pasti et al. 1997; Wang et al. 2006). Such a $[Ca^{2+}]_i$ increase triggers release of a variety of signaling substances, including glutamate, purines, D-serine, eicosanoids, and tumor necrosis factor alpha (TNF-α) (Volterra and Meldolesi 2005). Evidence suggests that glutamate and D-serine are released from astrocytes via Ca^{2+}-dependent exocytosis (for review, see Oliet and Mothet 2008; Santello and Volterra 2009). The existence of a tightly regulated mechanism of glutamate release in astrocytes (Bezzi et al. 2004; Marchaland et al. 2008) is consistent with data indicating that these cells play rapid and precise roles in neuromodulation (Jourdain et al. 2007; Perea and Araque 2007; Santello et al. 2011) and neurovascular coupling (Winship et al. 2007; Schummers et al. 2008). However, conflicting data have been presented (Fiacco et al. 2007; Li et al. 2008; Petravicz et al. 2008; Agulhon et al. 2010), questioning the existence of rapid gliotransmitter exocytosis from astrocytes serving physiological neuromodulation (Agulhon et al. 2008; Fiacco et al. 2009). To resolve this controversy, there is a need to provide direct in situ evidence of glutamate-containing vesicles in adult astrocytes. As for D-serine, data suggest that this amino acid is released from astrocytes to act as an endogenous N-methyl-D-aspartate (NMDA) receptor co-agonist at central synapses (Panatier et al. 2006; Oliet and Mothet 2008, but see Rosenberg et al. 2010). Moreover, astrocyte D-serine was recently found to be essential for the establishment of NMDA receptor–dependent long-term potentiation (LTP) in the hippocampus (Henneberger et al. 2010). However, it is not known whether D-serine is stored in vesicles of astrocytes in situ, although in vitro evidence indicates that D-serine and glutamate could be contained in similar vesicular organelles (Martineau et al. 2008). Here, we address these questions by using high-resolution quantitative immunogold cytochemistry with specific antibodies to glutamate and D-serine.

Materials and Methods

Perfusion Fixation and Antibody Specificity

Rats derived from the Wistar strain (4–5 weeks) were anesthetized with pentobarbital (100 mg/kg) before fixation through transcardiac perfusion (50 mL/min for 15 min) with a mixture of 4% formaldehyde and 0.5% glutaraldehyde (glutamate/EEAT2, glutamate/VGLUT1, and D-serine/VGLUT1 immunocytochemistry, n = 3 rats) or 2.5% glutaraldehyde and 1% formaldehyde (D-serine/EAAT2 and glutamate/D-serine immunocytochemistry, n = 3 rats or morphological analysis, n = 3 rats). For morphological analysis, the fixed tissues were treated with 1% osmium tetroxide before embedding in Durcupan. For immunogold analysis, specimens of hippocampus were cryoprotected with increasing concentrations of glycerol (10%, 20%, and 30%) and embedded in Lowicryl HM20 according to a freeze substitution protocol. Ultrathin sections (50–100 nm) were subjected to either morphological analysis or postembedding immunogold cytochemistry (Bergersen et al. 2008) using the following primary antibodies: rabbit anti-glutamate (no 607, dilution 1:30 000), rabbit anti-D-serine (no 21 236, dilution 1:2000), rabbit anti-EAAT2 (a mixture of anti-B12, 10 μg/mL and anti-B493, 5 μg/mL), goat anti-EAAT2 antibodies (2 μg/mL, Santa Cruz Biotechnology, Santa Cruz, CA), guinea pig anti-VGLUT1 antibodies (dilution 1:1000 Synaptic Systems), mouse caveolin-1 antibodies (dilution 1:300, BD Biosciences), rabbit anti-calreticulin antibodies (dilution 1:300, AbCam), and mouse anti-glutamine syntehase antibodies (dilution 1:100, BD Biosciences). The anti-glutamate and anti-D-serine antibodies were raised essentially as first described (Storm-Mathisen et al. 1983). The 607 glutamate antiserum has been proven to be specific through extensive characterization (Broman et al. 1993; Gundersen et al. 1998) and was used with the addition of 0.2 mM glutaraldehyde- and formaldehyde-treated aspartate and glutamine. The 21 236 D-serine antiserum has not been characterized previously. To test the D-serine antibodies, test specimens (Ottersen and Storm-Mathisen 1984) were made by spotting conjugates of about 50 different amino acids and peptides endogenous to the brain, linked to brain proteins by glutaraldehyde/formaldehyde onto cellulose nitrate/acetate filters. The test filters were processed with the D-serine antibodies according to a 3 layer peroxidase–antiperoxidase method. The tested compounds were L- and D-serine, L- and D-homocysteate, D-cysteine, DL-homocysteine, L-citrulline, reduced glutathione, β-alanine, D-aspartate, hypotaurine, L-cystine, L-isoleucine, D-arginine, L-methionine, glutamyl-glutamate, D-leucine, L-phenylalanine, L-serine, null (no amino acid), L-leucine, L-proline, γ-aminobutyric acid (GABA), L-glutamate, L-taurine,

glycine, L-aspartate, L-glutamine, epinephrine, norepinephrine, phosphoetanolamine, 3-aminopropane sulphonate (homotaurine), L-homocysteine sulphinate, L-α-alanine, L-valine, L-tryptophane, L-threonine, L-cysteine, L-tyrosine, L-asparagine, L-lysine, L-arginine, L-histidine, L-cysteate, glutamyltaurine, cysteine sulphinate, N-acetylaspartate, oxidized glutathione, L-S-sulpho-cysteine, leu-enkephalin, and met-enkephalin. There was a slight cross-reactivity against L-serine as well as against L-cysteine, which disappeared when the serum was preabsorbed with soluble glutaraldehyde/formaldehyde complexes of these amino acids. In each immunogold experiment, ultrathin test sections (Ottersen 1987) were processed along with the hippocampal sections, ascertaining the specificity of the labeling produced. The test sections were made of conjugates of different amino acids linked to brain macromolecules by glutaraldehyde–formaldehyde, which were freeze dried and embedded in epoxy resin (Ottersen 1987). In particular, the D-serine antibodies were tested against 12 different amino acids (D-serine, L-cystein, D-cystein, L-valine, α-alanine, glycine, L-serine, L-glutamate, L-aspartate, glutamine, GABA, and taurine) of which only the conjugate-containing D-serine was labeled (see Supplementary Fig. 1).

We also tested the rabbit 87554 D-serine antiserum, which showed quite a strong labeling of the D-serine conjugate but also an additional weak labeling of all the other amino acid conjugates in the electron microscopic "test sandwich." Thus, in this project, we only used the 21 236 D-serine antiserum. In the course of the experiments, we tested 2 commercial rabbit anti-D-serine antisera, one from AbCam (ab 6572; Cambridge, UK) and one from Advanced Targeting Systems (AB-T048; San Diego, CA). Both antibodies produced a strong cross-reactivity against the GABA conjugate in the ultrathin test sections as well as strong labeling of terminals forming symmetrical synapses in the ultrathin tissue sections (not shown). As an extra negative control test, the glutamate and D-serine immunoreactivities of tissue and test sections were blocked by adding 0.3 mM aldehyde-treated glutamate and D-serine to the respective antisera. The rabbit EAAT2 antisera (anti-B12 and anti-B493) have been extensively characterized (Lehre et al. 1995; Beckstrøm et al. 1999). When tested on western blots of hippocampal homogenates, the VGLUT1 antibodies produced a single band with an appropriate molecular weight of about 65 kDa. In a parallel study, the VGLUT1 antibodies produced strong astrocytic labeling in wild type and weak labeling in VGLUT1 knockout hippocampus (L Ormel, LH Bergersen, V Gundersen, unpublished data). According to the manufacturer, the caveolin-1, calreticulin, and glutamine synthetase antibodies are specific and give one single band with appropriate molecular weights on western blots of brain tissue.

The rabbit glutamate, rabbit D-serine, and rabbit calreticulin primary antibodies were visualized with goat anti-rabbit (10 nm gold particles, BBI, UK), the rabbit EAAT2 antibodies with goat anti-rabbit (15 nm gold particles, BBI), the goat EAAT2 antibodies with donkey anti-goat (15 nm gold particles, Aurion, the Netherlands), the guinea pig VGLUT1 antibodies with goat anti-guinea pig (15 nm gold particles, BBI), the mouse glutamine synthetase antibodies with goat anti-mouse (15 nm gold particles, BBI), and the mouse caveolin-1 antibodies with goat anti-mouse (10 nm gold particles, BBI) secondary antibodies. In double labeling immunogold experiments, in which the rabbit EAAT2 antibodies were used, glutamate- or D-serine–labeled sections were treated with formaldehyde vapor (70 °C, 1 h) to inactivate unoccupied binding sites on the primary rabbit immunoglobulins, before labeling with the rabbit anti-EAAT2 antibodies. The same approach was used in double labeling for D-serine and glutamate (visualized with the 10 and 15 nm coupled goat anti-rabbit secondary antibodies, respectively). The rabbit anti-EAAT2 and goat EAAT2 antibodies showed similar immunogold labeling patterns. In the quantitative analysis (see below), we used sections that were labeled with the glutamate or D-serine antibodies in the first step and the rabbit EAAT2 antibodies in the second step.

Morphological and Quantitative Immunogold Analysis

Electron micrographs of the ultrathin tissue sections were randomly taken (with a Philips CM 10 or a Tecnai 12 electron microscope) in the outer two-thirds of the dentate molecular layers, which are the termination fields for the perforant path glutamatergic afferents (Amaral and Witter 1989). All quantifications were done on micrographs magnified at ×46 000.

Morphological Analysis

For the morphological analysis, astrocytic processes surrounding asymmetric synapses between nerve terminals and dendritic spines were identified according to published criteria (Peters et al. 1991; Lehre and Danbolt 1998; Ventura and Harris 1999) and by their concave shape and electron lucent appearance. Astrocytic processes included in the analysis had cross-sectional diameters below 800 nm. When the morphological analysis was performed in Lowicryl-embedded tissue, astrocytic processes were also identified by labeling of EAAT2 (Chaudhry et al. 1995; Bezzi et al. 2004). Round and clear vesicular structures in perisynaptic astrocytic processes were included in the analysis if they had a diameter between 20 and 80 nm. The perpendicular distance from the astrocytic plasma membrane to the centers of synaptic-like microvesicles (SLMVs) in astrocytic processes was analyzed and frequency histograms made. The number of synaptic vesicles (SVs) in nerve terminals and SLMVs in astrocytic processes were counted. The areas of nerve terminals and astrocytic processes, as well as of clusters of SVs and SLMVs, were determined by point counting using an overlay screen (Bergersen et al. 2008), and the densities of SVs and SLMVs calculated. The cluster of SVs in nerve terminals was recorded over an area made up by the presynaptic active zone and perpendicular lines (distance of 100 nm) drawn from the end of the active zone; and the cluster of SLMVs in astrocytic processes was recorded over an area made by outlining of the grouped SLMVs (exemplified in Fig. 1 and Supplementary Fig. 2).

In addition, to investigate whether the SLMVs are randomly distributed throughout the process or show a regularly spaced organization, a plugin for ImageJ (http://rsb.info.nih.gov/ij/) was used to outline the plasma membrane of the astrocytic process and record the locations of the centers of SLMVs in the profile. Random points (similar numbers as the numbers of SLMVs in the profiles) were placed over the astrocytic profiles 49 times in succession. Recorded coordinates were submitted to a program written in Python (http://www.python.org) for computation of clusters of SLMVs and random points. An SLMV or a random point was defined as belonging to a cluster if their centers were situated <100 nm from the closest SLMV or random point (see Supplementary Result 1). The distances between the clusters of SLMVs and random points were calculated in the following way: first, perpendicular lines from the cluster centers were drawn to the astrocytic plasma membrane. Then, the distances along the plasma membrane between each SLMV and random point intersection with the plasma membrane were calculated. The statistical significance of the difference between the observed and expected (random points) distributions among bins was evaluated by the chi-square test for known distributions (see Supplementary Result Fig. 1).

Glutamate and D-serine Quantifications

For immunogold quantifications of glutamate and D-serine, only the astrocytic processes (identified by morphological criteria) with visible EAAT2-positive plasma membranes that surrounded excitatory synapses were included in the study. EAAT2 has been shown to be selectively located in astrocytic membranes (Chaudhry et al. 1995). A synapse was defined as excitatory when it contained an asymmetric synaptic specialization and/or high levels of glutamate in the presynaptic terminal (above twice the glutamate levels in dendrites). Glutamate and D-serine immunogold particles and grid points for area determination (see below) were recorded over SLMVs in EAAT2-positive astrocytic processes, over SVs in excitatory nerve terminals, and over cytoplasmic matrix (areas free of vesicles and mitochondria in the astrocytes and nerve terminals). SLMVs and SVs were included in the analysis if they had a diameter ranging from 20 to 80 nm (this study, Gundersen et al. 1998; Bezzi et al. 2004). As the lateral resolution of the current immunogold method (Supplementary Fig. 3) is similar to the diameter of the SLMVs, the method cannot localize a gold particle to a single vesicle. Thus, epitopes within SVs may be signaled by gold particles outside the vesicles and vice versa. To bypass this problem, gold particles were ascribed to the SLMVs and SVs if the particle centers were inside the vesicles or located in the cytoplasmic matrix within a 30 nm distance from the outer border of the vesicles. This is a distance within which most of the immunogold particles are expected to occur. Details of these criteria are given in Supplementary

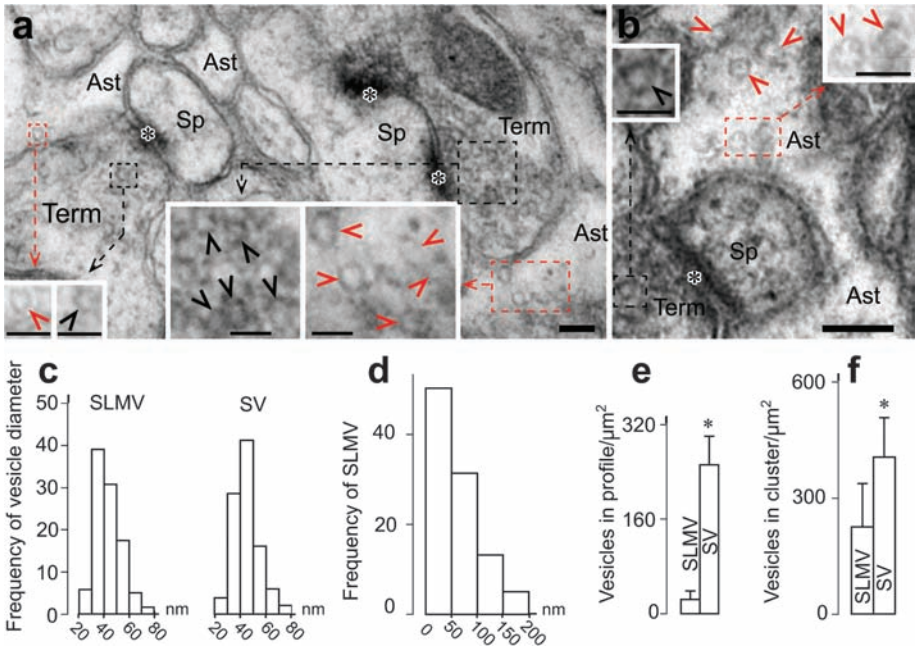

Figure 1. Astrocytic processes facing asymmetric synapses in the dentate molecular layer contain SLMVs. (*a* and *b*) Electron micrographs of osmicated tissue embedded in epoxy resin showing astrocytic processes (Ast), containing small and clear SLMVs with an oval/round shape that are close to the plasma membrane. Insets: Higher magnification of SLMVs (red arrowheads) and SVs (black arrowheads). In (*b*), red dotted lines highlight a small cluster of SLMVs (other examples in Supplementary Fig. 1). Symbols: Term, nerve terminal; Sp, dendritic spines; stars, synaptic clefts. Scale bars: 100 and 50 nm in insets. (*c*) Comparative frequencies of SLMV and SV diameters. Diameters were sorted into bins of 20 nm (columns, *x* axis) and the percentage of total calculated for each bin (*y* axis). The mean diameter ± SD of the SLMVs (36.6 ± 10.8 nm, $n = 241$ vesicles in 48 processes) and SV (39.2 ± 11.4 nm, 333 vesicles in 8 nerve terminals). (*d*) Histogram showing the frequency of SLMVs (indicated along *y* axis) related to their distance (nm) from the astrocytic plasma membrane (indicated along *x* axis). The distances between the center of the vesicles and the astrocytic plasma membrane were put into bins of 50 nm. (*e* and *f*) Bar charts showing the vesicle density (average number of SLMVs and SVs/µm² ± SD) either in the entire astrocytic process ($n = 48$) and nerve terminal ($n = 18$) profiles or specifically in vesicle clusters in astrocytic processes ($n = 48$) and in the synaptic vesicle pool located <100 nm from the nerve terminal active zone ($n = 18$) (see also Supplementary Fig. 1). *, the value for SV is significantly higher than the value for SLMV ($P < 0.01$, Mann–Whitney *U* test, two tails).

Figure 3 (see also Chaudhry et al. 1995; Matsubara et al. 1996). Using this criterion, a gold particle was ascribed to a vesicle if the center of the particle was located within an area defined by a boundary drawn 30 nm from the vesicle membrane (see Supplementary Fig. 3). Particles located outside of this "vesicle area" were assigned to the cytoplasmic matrix. To correct for the contamination of the vesicle labeling with the cytoplasmic matrix labeling, the gold particle densities recorded over cytoplasmic matrix were subtracted from the gold particle densities recorded for the vesicles. The areas of the profiles included in the analysis were determined by point counting using an overlay screen (Bergersen et al. 2008). The densities of glutamate and D-serine immunogold particles (average number of gold particles/square micrometer) in the different tissue profiles were calculated, and the results statistically evaluated by a nonparametric test (Mann–Whitney *U*, Statistica). To sum up, we counted the number of glutamate and D-serine gold particles belonging to individual vesicles and estimated the total area that individual vesicles occupy in a profile, thus obtaining a measure of the density of gold particles per vesicle area.

The spatial relationships between gold particles signaling: 1) D-serine (10 nm) or glutamate (10 nm) and VGLUT1 (15 nm); 2) D-serine (10 nm) and glutamate (15 nm); and 3) calreticulin (10 nm) or caveolin-1 (10 nm) and VGLUT1 (15 nm) in morphologically identified astrocytic processes and excitatory nerve terminals were determined by a computer program (http://rsb.info.nih.gov/ij/). The intercenter distances between the 10 and 15 nm gold particles were calculated, and the distances were sorted into bins of 20 nm. The frequency distributions were evaluated by a chi-squared test (Statistica).

The relationship between the density of glutamate and D-serine immunogold particles and the concentration of fixed glutamate and D-serine in the tissue was close to linear, as assessed by simultaneously processed test sections with conjugates containing known concentrations of glutamate (Ottersen 1989a) and D-serine (see Supplementary Fig. 4). Similar relationships between the density of gold particles signaling glutamate and the concentration of glutamate in the test conjugates as found in the present investigation have been described previously (Ottersen 1989a; Bramham et al. 1990). The D-serine–graded test conjugates were made as previously described for graded D-aspartate sections (Gundersen et al. 1995). In brief, slabs of 7% gelatin and 10% human serum albumin (HSA) with known areas were incubated in 10% HSA at various concentrations of D-serine (0, 0.33, 1, 3, 9, and 27 mM) before immersing in the tissue fixative (2.5% glutaraldehyde and 1% formaldehyde) for 1 h. The fixed blocks were then embedded in Durcupan. The concentrations of D-serine in the conjugate slabs after fixation (but before embedding) were determined by liquid scintillation counting using tracer amounts of D-^{3}H-serine (Perkin Elmer). Hence, the particle density in tissue compartments could be compared with those over the different D-serine conjugates.

Results

Synaptic-Like Microvesicles

We analyzed astrocytes in the hippocampal dentate molecular layer of adult rats. At first, we used a preparation optimized for morphologic visualization of membrane-bounded structures (tissue fixed with high glutaraldehyde concentration, postfixed with osmium tetroxide, and embedded in epoxy resin) to quantify vesicular organelles in delicate astrocytic processes surrounding excitatory synapses. The perisynaptic astrocytic processes (average cross-sectional diameters of 429 ± 195 nm [standard deviation {SD}, $n = 48$]) were identified by their concave shape and low electron density (Lehre and Danbolt 1998). Figure 1 shows that these processes contain vesicles resembling SVs. They are small (average diameter of about 36 nm, Fig. 1*c*), clear, and round/oval, justifying the term SLMV

(Bezzi et al. 2004; Jourdain et al. 2007). The SLMVs were found to be present in the majority (67%) of the observed processes, with a nonrandom distribution throughout the cytoplasm. They were situated in small clusters of 2–15 vesicles (Figs 1*a,b* and 2) and were preferentially located at or near the astrocytic plasma membrane (maximal frequency within 50 nm from the membrane, Fig. 1*d*). In profiles containing more than one cluster, the average intergroup distance was 340 ± 209 nm (SD, $n = 350$ clusters). The average density of SLMVs in an astrocytic profile was about one-tenth of the density of SVs in excitatory terminals (Fig. 1*e*), but within the area delimiting an astrocytic cluster, the density of SLMVs was about one-half of the density of SVs located in proximity (within 100 nm) of the presynaptic membrane active zone (Figs 1*f* and 2; for detailed quantitative analysis of SLMVs in perisynaptic processes, see Supplementary Result 1).

Quantitative Immunogold Cytochemistry

We then continued our investigations on tissue prepared for optimal immunogold sensitivity (tissue treated with uranyl acetate and embedded in Lowicryl). In this case, astrocytic processes were identified and selected for analysis not only according to the morphological criteria indicated above but also based on the membrane labeling for the astrocytic glutamate transporter EAAT2/GLT1. Small clusters of SLMVs located at or near the astrocytic membrane (Supplementary Fig. 2) were visible also in this preparation, and individual vesicles could be reliably recognized (Supplementary Result 2), even though their membranes were less distinct than the SV membranes. We therefore tested whether SLMVs contain glutamate and D-serine by use of specific antibodies against the 2 amino acids. The protocol for attributing glutamate and D-serine immunogold particles to vesicles or to the cytoplasmic matrix is given in Materials and Methods (section on morphological and immunogold analysis). Using this approach, we could show that astrocytic SLMVs contain immunogold particles signaling glutamate and D-serine (Fig. 2). This conclusion was reinforced by the observation that most of the immunogold particles signaling glutamate and D-serine were located <100 nm from the astrocytic plasma membrane and followed the SLMV distribution (Supplementary Fig. 5).

The density of glutamate immunogold particles over the SLMVs was much higher than the density in the cytoplasmic matrix of the astrocytes and only slightly lower than the density over SVs in adjacent excitatory nerve terminals. The particle density in the cytoplasmic matrix of the astrocytes was, in turn, lower than that in the cytoplasmic matrix of nerve terminals (Fig. 2*a–c*). To assess the degree of glutamate accumulation in the vesicles, we calculated the ratio of glutamate labeling between the vesicles and the cytoplasmic matrix. This ratio was higher between SLMV/astrocytic cytoplasmic matrix than between SVs/terminal cytoplasmic matrix (22 vs. 6; see Supplementary Result 3 for a control of the fixation efficiencies of free amino acids at protein-rich vs. nonprotein-rich sites in the tissue).

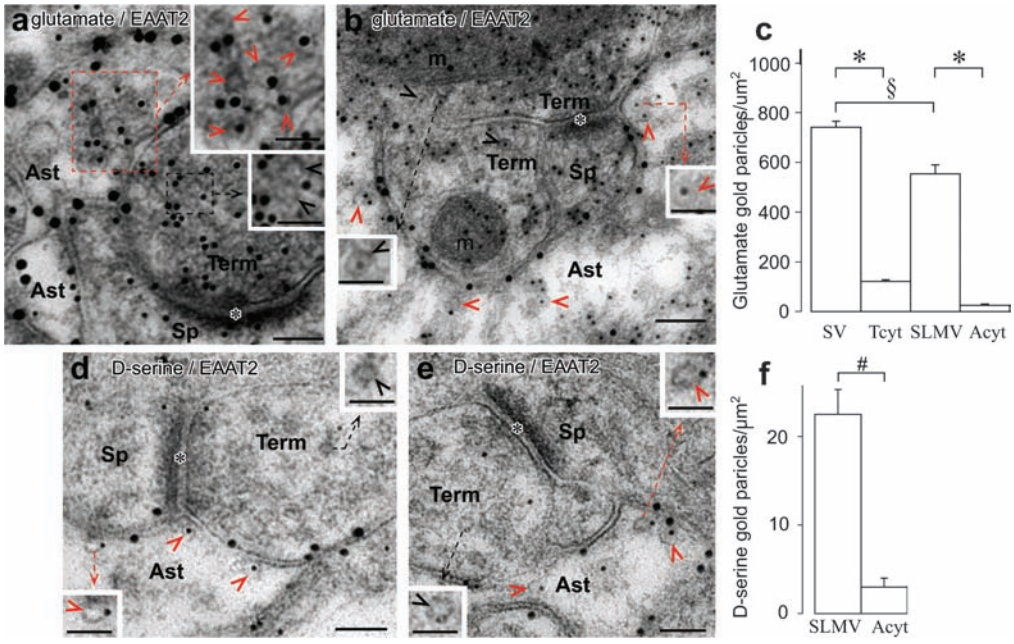

Figure 2. Glutamate and D-serine are located in SLMVs in astrocytic processes in the dentate molecular layers. (*a–b* and *d–e*) Electron micrographs showing examples of glutamate (*a–b*) and D-serine (*d–e*) labeling (small gold particles) of SLMVs (some indicated by red arrowheads) in astrocytic processes (Ast) positive for EAAT2 (large gold particles). Gold particles signaling glutamate are also located over synaptic vesicles (some indicated by black arrowheads) in asymmetric synapses (stars) between nerve terminals (Term) and dendritic spines (Sp). Insets: higher magnification showing the similarities between SLMVs (red dotted arrows) and SVs (black dotted arrow). Note that the astrocytic SLMVs are often localized in small clusters close to the plasma membrane. *a–b* show tissue fixed in low glutaraldehyde, while *d–e* show tissue fixed in high glutaraldehyde. Scale bars: 100 and 50 nm in insets. m: mitochondria. (*c* and *f*) Immunogold quantification of glutamate (*c*) and D-serine (*f*) gold particles in astrocytic processes. The bar charts show the mean number of glutamate and D-serine gold particles/μm^2 ± SD in SLMVs and the cytoplasmic matrix of astrocytic processes (Acyt) in $n = 3$ animals. In addition, we show the density of glutamate gold particles in nerve terminals over SVs and the cytoplasmic matrix (Tcyt). Background glutamate and D-serine labeling over empty resin (0.9 and 0.8 gold particles/μm^2, respectively) were subtracted. The numbers of astrocytic processes and nerve terminals included in the glutamate analysis from each animal were 44–50 and 13–21, respectively, while the numbers of astrocytic processes included in the D-serine analysis from each animal were 25–28. *, the glutamate values in SV and SLMV are significantly higher than the values in Tcyt and Acyt, respectively ($P < 0.001$, Mann–Whitney *U* test, two tails). §, the glutamate value in SV is significantly higher than the value in SLMV ($P < 0.05$, Mann–Whitney *U* test, 2 tails). #, the D-serine value in SLMV is significantly higher than the value in Acyt ($P < 0.001$, Mann–Whitney *U* test, two tails).

As previously reported, D-serine labeling was observed in astrocytic processes (Schell et al. 1995; Williams et al. 2006) (Fig. 2*d,e*). Gold particles representing D-serine were associated with the SLMVs rather than with the cytoplasmic matrix (Fig. 2*f*). The ratio of D-serine gold particle density between SLMV and cytoplasmic matrix of the astrocytes was 8, suggesting a considerable accumulation of D-serine in the SLMVs. In addition, nerve terminals exhibited a rather weak D-serine signal with no clear association to vesicular structures (Kartvelishvily et al. 2006) (for details of the intraterminal distribution of D-serine, see Supplementary Result 4).

The approximate concentration of glutamate and D-serine in the different tissue profiles was estimated by calibration with known concentrations of glutamate and D-serine (see Supplementary Fig. 4). The glutamate gold particle densities corresponded to a concentration of glutamate of ~50–60 mM in SLMVs and SVs and of ~2 and ~10 mM in the cytoplasmic matrix of the astrocytes and the nerve terminals, respectively. For D-serine, we estimated that the concentration of fixed D-serine in the SLMVs was ~10 mM, whereas the D-serine concentration in the astrocyte cytoplasmic matrix was ~1 mM.

To investigate whether glutamate and D-serine are contained in the same pool of SLMVs, we performed double labeling with the glutamate and D-serine antibodies. In none of the investigated astrocytic processes was there any clear evidence of colocalization of the 2 amino acids in the same SLMV (Fig. 3*a,e*). Likewise, colabelling with D-serine and VGLUT1 antibodies did not reveal any clear colocalization (Fig. 3*b,f*), whereas, as expected, there were several examples of glutamate and VGLUT1 gold particles associated with the same SLMV as well as with SVs (Fig. 3*c,g,* and *h*). It should, however, be noted that the D-serine and VGLUT1 antibodies produced a relatively low immunolabeling of SLMVs, which could have led to an underestimation of D-serine/glutamate and D-serine/VGLUT1 double labeling. Thus, we cannot totally exclude a partial colocalization of D-serine and glutamate in the same vesicle pool.

Exocytosis of SLMVs in astrocytes has been proposed to occur upon Ca^{2+} mobilization from the endoplasmic reticulum (ER) (Marchaland et al. 2008). We checked the presence of ER tubules in the perisynaptic astrocytic processes and their spatial relation with SLMVs. Antibodies against the ER marker calreticulin labeled elongated tubular structures, mostly in

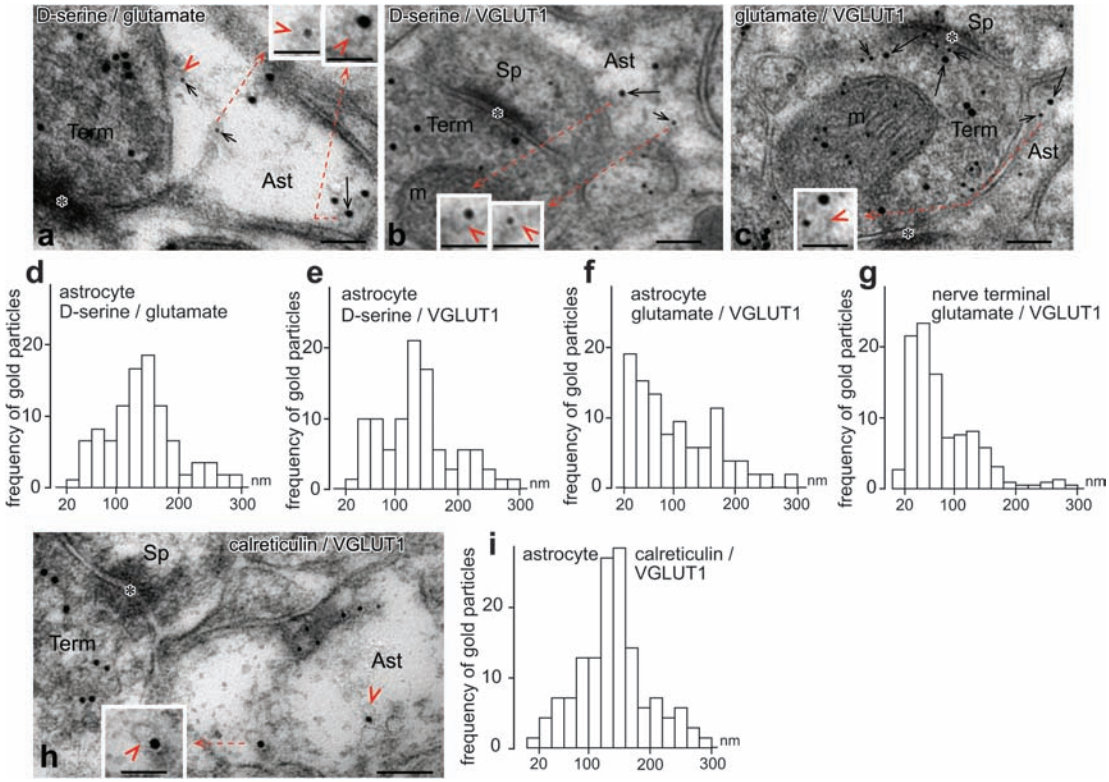

Figure 3. SLMVs containing glutamate do not coincide with SLMVs containing D-serine: spatial association with ER in astrocytic processes. (*a–c* and *h*) Double labeling of D-serine (small gold particles)/glutamate (large gold particles) (*a*), D-serine (small gold particles)/VGLUT1 (large gold particles) (*b*), glutamate (small gold particles)/VGLUT1 (large gold particles) (*c*), and calreticulin (small gold particles)/VGLUT1 (large gold particles) (*d*) at excitatory synapses between nerve terminals (Term) and postsynaptic spines (Sp) surrounded by astrocytic processes (Ast) in the dentate molecular layer. Short arrows indicate D-serine in *a–b*, glutamate in *c*, and calreticulin in *h*. Long arrows indicate glutamate in *a* and VGLUT1 in *b–c* and *h*. The SLMVs are indicated by red arrowheads. The insets show higher magnification of SLMVs positive for either glutamate or D-serine (*a–b*), for both glutamate and VGLUT1 (*c*), and for VGLUT1 (*h*). m = mitochondria. Scale bars: 100 and 50 nm in insets. (*d–g* and *i*) Distances separating gold particles signaling: D-serine/glutamate (*d*) and D-serine/VGLUT1 (*e*) in astrocytic processes; glutamate/VGLUT1 in astrocytic processes (*f*) and nerve terminals (*g*); calreticulin/VGLUT1 in astrocytic processes (*i*). Distances are put into bins of 20 nm (columns, *x* axis), and the percent of total in each bin is given along the *y* axis. Because of the diameter of the vesicle (30–40 nm) and the lateral resolution of the immunogold method (~30 nm), gold particles signaling 2 different epitopes in the same vesicle could be separated by a distance of up to about 90–100 nm. Most of the D-serine/glutamate or D-serine/VGLUT1 and calreticulin/VGLUT1 gold particles do not signal epitopes in the same vesicular membrane, while most of the gold particles representing glutamate/VGLUT1 belong to the same vesicle. The distribution of D-serine/glutamate, D-serine/VGLUT1, and calreticulin/VGLUT1 intercenter distances was significantly different from the glutamate/VGLUT1 distribution ($P < 0.01$, chi-squared test). These quantifications were done in 25 astrocytic processes positive for D-serine/glutamate, in 25 astrocytic processes positive for D-serine/VGLUT1, in 23 astrocytic processes and 27 nerve terminals positive for glutamate/VGLUT1, and in 20 astrocytic processes positive for calreticulin/VGLUT1 in one animal, but similar results were obtained in 2 other animals.

neuronal dendritic profiles, but also in astrocytic processes (Fig. 3*d*,*i*; Supplementary Fig. 6). VGLUT1 and calreticulin double labeling suggest that the astrocytic processes are equipped with ER located close to (within 100–200 nm), but not overlapping with, glutamate-containing SLMVs (Fig. 3*d*). Astrocytic processes were also endowed with membrane-bounded structures labeled for caveolin-1. Double labeling for VGLUT1 and caveolin-1 (Supplementary Fig. 7) showed no significant colocalization, suggesting that astrocytic processes contain several pools of vesicle-like organelles that may serve separate functions, such as storage of transmitters, storage of Ca^{2+}, and caveola-mediated endocytosis.

Discussion

The present immunogold data from perisynaptic astrocytic processes provide the first direct evidence that the putative gliotransmitters glutamate and D-serine are stored in astrocytic SLMVs in situ in the adult brain. The presence in the fine perisynaptic processes of clusters of transmitter-containing SLMVs at or near the astrocytic membrane, together with spatially related ER tubules, is a prerequisite for precise astrocyte-to-neuron communication. Indeed, these ultrastructural observations support functional data showing that activation of endogenous G protein-coupled receptors on astrocytes induces glutamate receptor–dependent and tetanus toxin sensitive presynaptic modulation in situ (Jourdain et al. 2007; Perea and Araque 2007) and that astrocytes display a glutamate exocytosis process tightly regulated by TNF-α (Santello et al. 2011). Moreover, our data are in line with the recent observation that selective dialysis of tetanus toxin in astrocytes prevents LTP induction at neighboring synapses by blocking D-serine release (Henneberger et al. 2010). Tetanus toxin is an exocytosis blocker acting on VAMP3/cellubrevin, which is expressed in SLMVs (Bezzi et al. 2004). The present and previous observations in support of astrocytic transmitter exocytosis were made in the hippocampus. However, the conclusions are likely to be more generally valid as VGLUT1 is closely associated with SLMVs also in several other brain regions, including frontal cortex and striatum (L Ormel, LH Bergersen, V Gundersen, unpublished data). It should also be noted that in freshly isolated astrocytes, recent observations show that, unlike lysosomal vesicles, small vesicles in astrocytes exocytose glutamate in a vesicular glutamate transporter–dependent manner (Liu et al. 2011), which is in strong support of our data on glutamate localization in astrocytic SLMVs.

Our present data also reveal an important number of similarities between glutamate-containing SLMVs in astrocytic processes and SVs in excitatory nerve terminals. Not only are SLMVs similar to SVs in size and shape, as previously reported (Bezzi et al. 2004), but also in glutamate content, which is here estimated in astrocytes for the first time, and in localization with respect to the astrocytic plasma membrane. Thus, most astrocytic SLMVs are as close to the plasma membrane as the readily releasable pool of SVs in nerve terminals (Gitler et al. 2004; Owe et al. 2009), consistent with the possibility that a proportion of astrocytic SLMVs is docked and competent for fast fusion in response to stimuli. The organization of SLMVs in astrocytic processes seems different from the grouping of a large SV population in nerve terminal structures. In particular, in the nerve terminals, there appears to be an accumulation of distinct pools of SVs, with a large reserve pool (80–90% of the vesicles) mostly located in the core region of the terminal and linked to the cytoskeleton by synapsin–actin interactions (Owe et al. 2009). Interestingly, hippocampal excitatory nerve terminals of synapsin-lacking mice display selective reduction in the density of this large pool, whereas the small readily releasable/recycling pool (<100 nm from the plasma membrane) remains largely intact (Gitler et al. 2004; Owe et al. 2009). The presence of distinct pools is not apparent in astrocytes, as SLMVs are all regrouped within 100 nm from the membrane, suggesting that astrocytes lack a defined reserve pool. This hypothesis seems plausible because mobilization of the reserve pool at synapses is triggered only during high-frequency neuronal activity. In astrocytes, exocytosis of SLMVs is evoked by activation of G protein–coupled receptors and even if the stimulus–secretion coupling can occur within 50–100 ms (Bezzi et al. 2004; Domercq et al. 2006; Marchaland et al. 2008), this signaling mode is not tailored for high-frequency encoding. Lack of a large reserve pool would explain both the significantly lower number of vesicles found in astrocytic processes compared with nerve terminals and their low electron density due to reduced protein–protein interactions. Moreover, we found that astrocytic processes are equipped with ER located close to glutamate-containing SLMVs. This subcellular arrangement could constitute a functional nanodomain in which local increases in Ca^{2+} concentration from the internal stores trigger release of glutamate from SLMVs (Marchaland et al. 2008). Ca^{2+} microdomains have been observed in astrocyte cultures (Lee et al. 2006; Shigetomi et al. 2010), and in addition to controlling transmitter release, it has been proposed that such domains may be involved in local volume regulation in astrocytes (Akita and Okada 2011). In the cerebellum, neuronal stimulation has been shown to trigger Ca^{2+} increase in Bergmann glial cells at distinct microdomains (Grosche et al. 1999). Moreover, very recent evidence in the adult dentate gyrus shows that astrocytic processes respond to local synaptic events with highly confined Ca^{2+} elevations that, in turn, participate to the control of transmitter release at local synapses (Di Castro et al. 2011), strongly supporting the view that these astrocyte domains represent local sites at which astrocyte-neuron signaling occurs.

The present study provides estimated values of the vesicular and cytosolic glutamate concentrations in nerve terminals and astrocytes. The values in SVs and in the cytoplasmic matrix of nerve terminals are in good agreement with previous estimates (Burger et al. 1989; Shupliakov et al. 1992). The glutamate concentration that we find in the cytosolic matrix of astrocytic processes is in the lower millimolar range, a concentration which can sustain glutamate uptake into SLMVs according to the reported Km of VGLUT-mediated vesicular uptake (Fremeau et al. 2004). As the glutamate ratios between vesicles and cytosolic matrix were different in nerve terminals and astrocytes, there may be some differences in the mechanisms regulating the filling of SLMVs and SVs. Indeed, mechanisms similar to those discovered to operate in dopaminergic (Brunk et al. 2006) and cholinergic (Gras et al. 2008) vesicles could contribute to regulate glutamate uptake into astrocytic SLMVs. An intriguing aspect of exocytosis regulation is whether VGLUTs are inserted into plasma membranes to function as phosphate transporters. However, we could not observe any immunogold signal for VGLUT1 in plasma membranes, neither in astrocytes nor in nerve terminals (LH Bergersen, V Gundersen, unpublished data).

Our findings regarding D-serine are intriguing. The labeling pattern in astrocytic processes strongly suggests a vesicular

localization of D-serine (see also Williams et al. 2006). However, the VGLUTs do not carry D-serine, suggesting that there is a vesicular transporter for D-serine that remains to be identified. D-serine is present in a population of astrocytic SLMVs structurally indistinguishable from the one storing glutamate. However, SLMVs containing D-serine and glutamate do not appear to overlap to any considerable extent. Yet, both glutamate-containing and D-serine–containing SLMVs are present in the same very fine astrocytic processes and are in the position of discharging their amino acid content into the perisynaptic area surrounding excitatory synapses on granule cell dendrites. It has been shown that glutamate released by exocytosis from astrocytes produces presynaptic NMDA receptor responses, which in turn strengthen the excitatory synaptic response at granule cell synapses (Jourdain et al. 2007, Santello et al. 2011). In addition, our results suggest that exocytosis underlies the astrocytic glutamate release detected by electrophysiology in stratum radiatum of CA1 hippocampus (Kang et al. 1998; Fiacco et al. 2004; Andersson et al. 2007; Andersson and Hanse 2010) and the cortex (Wirkner et al. 2007). There are several lines of evidence suggesting that release of D-serine from astrocytes can regulate neuronal NMDA receptors. In intact brain tissue, it is known that astrocytic D-serine release controls the level of activation of synaptic NMDA receptors and thereby long-term synaptic signaling in the hypothalamus (Panatier et al. 2006) and CA1 hippocampus (Henneberger et al. 2010). Likewise, in the retina, it is known that glial cell–derived D-serine can enhance NMDA receptor responses (Stevens et al. 2003). Using a combination of neurons and astrocytes in culture and hippocampal slices, Yang et al. (2003) found that D-serine released from astrocytes enhanced neuronal NMDA receptor currents and triggered LTP. Interestingly, the release of D-serine from astrocytes can be subjected to regulation, for example, by ephrinBs (Zhuang et al. 2010).

In conclusion, we propose that the joint or separate release of glutamate and D-serine from astrocytes could provide a sophisticated control of the activity of neuronal NMDA receptor populations.

Supplementary Material

Supplementary material can be found at: http://www.cercor.oxfordjournals.org/

Funding

Medical Faculty, University of Oslo, and the Norwegian Research Council; and Swiss National Science Foundation (3100A0-120398) to A.V.

Notes

Antibodies to EAAT2 were from N.C. Danbolt (University of Oslo, Norway). We thank B. Riber and K. M. Gujord for technical assistance with the D-serine antibodies. *Conflict of Interest* : None declared.

References

Agulhon C, Fiacco TA, McCarthy KD. 2010. Hippocampal short- and long-term plasticity are not modulated by astrocyte Ca^{2+} signaling. Science. 327:1250–1254.

Agulhon C, Petravicz J, McMullen AB, Sweger EJ, Minton SK, Taves SR, Casper KB, Fiacco TA, McCarthy KD. 2008. What is the role of astrocyte calcium in neurophysiology? Neuron. 59:932–946.

Akita T, Okada Y. 2011. Regulation of bradykinin-induced activation of volume-sensitive outwardly rectifying anion channels by Ca2+ nanodomains in mouse astrocytes. J Physiol. 589:3909–3927.

Amaral DG, Witter MP. 1989. The three-dimensional organization of the hippocampal formation: a review of anatomical data. Neuroscience. 31:571–591.

Andersson M, Blomstrand F, Hanse E. 2007. Astrocytes play a critical role in transient heterosynaptic depression in the rat hippocampal CA1 region. J Physiol. 585:843–852.

Andersson M, Hanse E. 2010. Astrocytes impose postburst depression of release probability at hippocampal glutamate synapses. J Neurosci. 30:5776–5780.

Beckstrøm H, Julsrud L, Haugeto O, Dewar D, Graham DI, Lehre KP, Storm-Mathisen J, Danbolt NC. 1999. Interindividual differences in the levels of the glutamate transporters GLAST and GLT, but no clear correlation with Alzheimer's disease. J Neurosci Res. 55:218–229.

Bergersen LH, Storm-Mathisen J, Gundersen V. 2008. Immunogold quantification of amino acids and proteins in complex subcellular compartments. Nat Protoc. 3:144–152.

Bezzi P, Gundersen V, Galbete JL, Seifert G, Steinhäuser C, Pilati E, Volterra A. 2004. Astrocytes contain a vesicular compartment that is competent for regulated exocytosis of glutamate. Nat Neurosci. 7:613–620.

Bramham CR, Torp R, Zhang N, Storm-Mathisen J, Ottersen OP. 1990. Distribution of glutamate like immunoreactivity in excitatory hippocampal pathways: a semiquantitative electron microscopic study in rats. Neuroscience. 39:405–417.

Broman J, Anderson S, Ottersen OP. 1993. Enrichment of glutamate-like immunoreactivity in primary afferent terminals throughout the spinal cord dorsal horn. Eur J Neurosci. 5:1050–1061.

Brunk I, Blex C, Rachakonda S, Höltje M, Winter S, Pahner I, Walther DJ, Ahnert-Hilger G. 2006. The first luminal domain of vesicular monoamine transporters mediates G-protein-dependent regulation of transmitter uptake. J Biol Chem. 281:33373–33385.

Burger PM, Mehl E, Cameron PL, Maycox PR, Baumert M, Lottspeich F, De Camilli P, Jahn R. 1989. Synaptic vesicles immunoisolated from rat cerebral cortex contain high levels of glutamate. Neuron. 3:715–720.

Chaudhry FA, Lehre KP, van Lookeren Campagne M, Ottersen OP, Danbolt NC, Storm-Mathisen J. 1995. Glutamate transporters in glial plasma membranes: highly differentiated localizations revealed by quantitative ultrastructural immunocytochemistry. Neuron. 15:711–720.

Dani JW, Chernjavsky A, Smith SJ. 1992. Neuronal activity triggers calcium waves in hippocampal astrocyte networks. Neuron. 8:429–440.

Di Castro MA, Chuquet J, Liaudet N, Bhaukaurally K, Santello M, Bouvier D, Tiret P, Volterra A. forthcoming 2011. Local Ca^{2+} detection and modulation of synaptic release by astrocytes. Nat Neurosci. doi: 10.1038/nn.2929.

Domercq M, Brambilla L, Pilati E, Marchaland J, Volterra A, Bezzi P. 2006. P2Y1 receptor-evoked glutamate exocytosis from astrocytes: control by tumor necrosis factor-alpha and prostaglandins. J Biol Chem. 281:30684–30696.

Fiacco TA, Agulhon C, McCarthy KD. 2009. Sorting out astrocyte physiology from pharmacology. Annu Rev Pharmacol Toxicol. 49:151–174.

Fiacco TA, Agulhon C, Taves SR, Petravicz J, Casper KB, Dong X, Chen J, McCarthy KD. 2007. Selective stimulation of astrocyte calcium in situ does not affect neuronal excitatory synaptic activity. Neuron. 54:611–626.

Fiacco TA, McCarthy KD. 2004. Intracellular astrocyte calcium waves in situ increase the frequency of spontaneous AMPA receptor currents in CA1 pyramidal neurons. J Neurosci. 24:722–732.

Fremeau RT, Jr, Voglmaier S, Seal RP, Edwards RH. 2004. VGLUTs define subsets of excitatory neurons and suggest novel roles for glutamate. Trends Neurosci. 27:98–103.

Gitler D, Takagishi Y, Feng J, Ren Y, Rodriguiz RM, Wetsel WC, Greengard P, Augustine GJ. 2004. Different presynaptic roles of synapsins at excitatory and inhibitory synapses. J Neurosci. 24:11368–11380.

Gras C, Amilhon B, Lepicard EM, Poirel O, Vinatier J, Herbin M, Dumas S, Tzavara ET, Wade MR, Nomikos GG, et al. 2008. The vesicular glutamate transporter VGLUT3 synergizes striatal acetylcholine tone. Nat Neurosci. 11:292–300.

Grosche J, Matyash V, Möller T, Verkhratsky A, Reichenbach A, Kettenmann H. 1999. Microdomains for neuron-glia interaction: parallel fiber signaling to Bergmann glial cells. Nat Neurosci. 2:139–143.
Gundersen V, Chaudhry FA, Bjaalie JG, Fonnum F, Ottersen OP, Storm-Mathisen J. 1998. Synaptic vesicular localization and exocytosis of L-aspartate in excitatory nerve terminals: a quantitative immunogold analysis in rat hippocampus. J Neurosci. 18:6059–6070.
Gundersen V, Shupliakov O, Brodin L, Ottersen OP, Storm-Mathisen J. 1995. Quantification of excitatory amino acid uptake at intact glutamatergic synapses by immunocytochemistry of exogenous D-aspartate. J Neurosci. 15:4417–4428.
Henneberger C, Papouin T, Oliet SH, Rusakov DA. 2010. Long-term potentiation depends on release of D-serine from astrocytes. Nature. 463:232–236.
Jourdain P, Bergersen LH, Bhaukaurally K, Bezzi P, Santello M, Domercq M, Matute C, Tonello F, Gundersen V, Volterra A. 2007. Glutamate exocytosis from astrocytes controls synaptic strength. Nat Neurosci. 10:331–339.
Kang J, Goldman SA, Nedergaard M. 1998. Astrocyte-mediated potentiation of inhibitory synaptic transmission. Nat Neurosci. 1:683–692.
Kartvelishvily E, Shleper M, Balan L, Dumin E, Wolosker H. 2006. Neuron-derived D-serine release provides a novel means to activate N-methyl-D-aspartate receptors. J Biol Chem. 281:14151–14162.
Lee MY, Song H, Nakai J, Ohkura M, Kotlikoff MI, Kinsey SP, Golovina VA, Blaustein MP. 2006. Local subplasma membrane Ca2+ signals detected by a tethered Ca2+sensor. Proc Natl Acad Sci U S A. 103:13232–13237.
Lehre KP, Danbolt NC. 1998. The number of glutamate transporter subtype molecules at glutamatergic synapses: chemical and stereological quantification in young adult rat brain. J Neurosci. 18:8751–8757.
Lehre KP, Levy LM, Ottersen OP, Storm-Mathisen J, Danbolt NC. 1995. Differential expression of two glial glutamate transporters in the rat brain: quantitative and immunocytochemical observations. J Neurosci. 15:1835–1853.
Li D, Ropert N, Koulakoff A, Giaume C, Oheim M. 2008. Lysosomes are the major vesicular compartment undergoing Ca2+-regulated exocytosis from cortical astrocytes. J Neurosci. 28:7648–7658.
Liu T, Sun L, Xiong Y, Shang S, Guo N, Teng S, Wang Y, Liu B, Wang C, Wang L, et al. 2011. Calcium triggers exocytosis from two types of organelles in a single astrocyte. J Neurosci. 31:10593–10601.
Marchaland J, Calì C, Voglmaier SM, Li H, Regazzi R, Edwards RH, Bezzi P. 2008. Fast subplasma membrane Ca^{2+} transients control exo-endocytosis of synaptic-like microvesicles in astrocytes. J Neurosci. 28:9122–9132.
Martineau M, Galli T, Baux G, Mothet JP. 2008. Confocal imaging and tracking of the exocytotic routes for D-serine-mediated gliotransmission. Glia. 56:1271–1284.
Matsubara A, Laake JH, Davanger S, Usami S, Ottersen OP. 1996. Organization of AMPA receptor subunits at a glutamate synapse: a quantitative immunogold analysis of hair cell synapses in the rat organ of Corti. J Neurosci. 16:4457–4467.
Oliet SH, Mothet JP. 2008. Regulation of N-methyl-D-aspartate receptors by astrocytic D-serine. Neuroscience. 158:275–283.
Ottersen OP. 1987. Postembedding light- and electron microscopic immunocytochemistry of amino acids: description of a new model system allowing identical conditions for specificity testing and tissue processing. Exp Brain Res. 69:167–174.
Ottersen OP. 1989a. Postembedding immunogold labelling of fixed glutamate: an electron microscopic analysis of the relationship between gold particle density and antigen concentration. J Chem Neuroanat. 2:57–66.
Ottersen OP, Storm-Mathisen J. 1984. Glutamate- and GABA-containing neurons in the mouse and rat brain, as demonstrated with a new immunocytochemical technique. J Comp Neurol. 229: 374–392.
Owe SG, Jensen V, Evergren E, Ruiz A, Shupliakov O, Kullmann DM, Storm-Mathisen J, Walaas SI, Hvalby Ø, Bergersen LH. 2009. Synapsin- and actin-dependent frequency enhancement in mouse hippocampal mossy fiber synapses. Cereb Cortex. 19:511–523.
Panatier A, Theodosis DT, Mothet JP, Touquet B, Pollegioni L, Poulain DA, Oliet SH. 2006. Glia-derived D-serine controls NMDA receptor activity and synaptic memory. Cell. 125:775–784.
Pasti L, Volterra A, Pozzan T, Carmignoto G. 1997. Intracellular calcium oscillations in astrocytes: a highly plastic, bidirectional form of communication between neurons and astrocytes in situ. J Neurosci. 17:7817–7830.
Perea G, Araque A. 2007. Astrocytes potentiate transmitter release at single hippocampal synapses. Science. 317:1083–1086.
Peters A, Palay SL, Webster H. 1991. The fine structure of the nervous system: the neurons and supporting cells. Philadelphia: W. B. Saunders.
Petravicz J, Fiacco TA, McCarthy KD. 2008. Loss of IP3 receptor-dependent Ca^{2+} increases in hippocampal astrocytes does not affect baseline CA1 pyramidal neuron synaptic activity. J Neurosci. 28:4967–4973.
Rosenberg D, Kartvelishvily E, Shleper M, Klinker CM, Bowser MT, Wolosker H. 2010. Neuronal release of D-serine: a physiological pathway controlling extracellular D-serine concentration. FASEB J. 24:2951–2961.
Santello M, Bezzi P, Volterra A. 2011. TNFα controls glutamatergic gliotransmission in the hippocampal dentate gyrus. Neuron. 69:988–1001.
Santello M, Volterra A. 2009. Synaptic modulation by astrocytes via Ca^{2+}-dependent glutamate release. Neuroscience. 158:253–259.
Schell MJ, Molliver ME, Snyder SH. 1995. D-serine, an endogenous synaptic modulator: localization to astrocytes and glutamate-stimulated release. Proc Natl Acad Sci U S A. 92:3948–3952.
Schummers J, Yu H, Sur M. 2008. Tuned responses of astrocytes and their influence on hemodynamic signals in the visual cortex. Science. 320:1638–1643.
Shigetomi E, Kracun S, Sofroniew MV, Khakh BS. 2010. A genetically targeted optical sensor to monitor calcium signals in astrocyte processes. Nat Neurosci. 13:759–766.
Shupliakov O, Brodin L, Cullheim S, Ottersen OP, Storm-Mathisen J. 1992. Immunogold quantification of glutamate in two types of excitatory synapse with different firing patterns. J Neurosci. 12:3789–3803.
Stevens ER, Esguerra M, Kim PM, Newman EA, Snyder SH, Zahs KR, Miller RF. 2003. D-serine and serine racemase are present in the vertebrate retina and contribute to the physiological activation of NMDA receptors. Proc Natl Acad Sci U S A. 100:6789–6794.
Storm-Mathisen J, Leknes AK, Bore AT, Vaaland JL, Edminson P, Haug FM, Ottersen OP. 1983. First visualization of glutamate and GABA in neurones by immunocytochemistry. Nature. 301:517–520.
Ventura R, Harris KM. 1999. Three-dimensional relationships between hippocampal synapses and astrocytes. J Neurosci. 19:6897–6906.
Volterra A, Meldolesi J. 2005. Astrocytes, from brain glue to communication elements: the revolution continues. Nat Rev Neurosci. 6:626–640.
Wang X, Lou N, Xu Q, Tian GF, Peng WG, Han X, Kang J, Takano T, Nedergaard M. 2006. Astrocytic Ca^{2+} signaling evoked by sensory stimulation in vivo. Nat Neurosci. 9:816–823.
Williams SM, Diaz CM, Macnab LT, Sullivan RK, Pow DV. 2006. Immunocytochemical analysis of D-serine distribution in the mammalian brain reveals novel anatomical compartmentalizations in glia and neurons. Glia. 53:401–411.
Winship IR, Plaa N, Murphy TH. 2007. Rapid astrocyte calcium signals correlate with neuronal activity and onset of the hemodynamic response in vivo. J Neurosci. 27:6268–6272.
Wirkner K, Günther A, Weber M, Guzman SJ, Krause T, Fuchs J, Köles L, Nörenberg W, Illes P. 2007. Modulation of NMDA receptor current in layer V pyramidal neurons of the rat prefrontal cortex by P2Y receptor activation. Cereb Cortex. 17:621–631.
Yang Y, Ge W, Chen Y, Zhang Z, Shen W, Wu C, Poo M, Duan S. 2003. Contribution of astrocytes to hippocampal long-term potentiation through release of D-serine. Proc Natl Acad Sci U S A. 100: 15194–15199.
Zhuang Z, Yang B, Theus MH, Sick JT, Bethea JR, Sick TJ, Liebl DJ. 2010. EphrinBs regulate D-serine synthesis and release in astrocytes. J Neurosci. 30:16015–16024.